Received: 14 July 2020 | Revised: 30 January 2021 | Accepted: 28 February 2021

DOI: 10.1111/ppl.13385

BIOCHEMISTRY AND METABOLISM

Physiologia Plantarum

Color variation in young and senescent leaves of Formosan sweet gum (*Liquidambar formosana*) by the gene regulation of anthocyanidin biosynthesis

Chi-Hsiang Wen[1] | Nai-Wen Tsao[2] | Sheng-Yang Wang[2] | Fang-Hua Chu[1]

[1]School of Forestry and Resource Conservation, National Taiwan University, Taipei, Taiwan

[2]Department of Forestry, National Chung-Hsing University, Taichung, Taiwan

Correspondence
Fang-Hua Chu, School of Forestry and Resource Conservation, National Taiwan University, Taipei, Taiwan.
Email: fhchu@ntu.edu.tw

Edited by E. Pesquet

Abstract

In certain plants, leaf coloration occurs in young and senescent leaves; however, it is unclear whether these two developmental stages are controlled by the same regulatory mechanisms. Formosan sweet gum (*Liquidambar formosana* Hance) is a subtropical deciduous tree species that possesses attractive autumnal leaf coloration. The color of young leaves is closer to purplish red, while senescent leaves are more orange-red to dark red. It was confirmed that delphinidin and cyanidin are the two anthocyanidins that contribute to the color of Formosan sweet gum leaves, and the content of different anthocyanins influences the appearance of color. To elucidate the regulation of anthocyanidin biosynthesis, recombinant DIHYDROFLAVONOL-4-REDUCTASEs (LfDFR1 and LfDFR2) (EC 1.1.1.234) were produced, and their substrate acceptability was investigated both *in vitro* and *in planta*. The functions of flavanones and dihydroflavonols modification by FLAVONOID 3′ HYDROXYLASE (LfF3′H1) (EC 1.14.14.82) and FLAVONOID 3′5′ HYDROXYLASE (LfF3′5′H) (EC 1.14.14.81) were verified using a transient overexpression experiment in *Nicotiana benthamiana*. The results showed that LfMYB5 induced *LfF3′5′H* and LfMYB123 induced both *LfF3′H1* and *LfDFR1* in spring when the leaves were expanding, whereas LfMYB113 induced *LfF3′H1*, *LfDFR1*, and *LfDFR2* in late autumn to winter when the leaves were undergoing leaf senescence. In conclusion, the color variation of Formosan sweet gum in young and senescent leaves was attributed to the composition of anthocyanidins through the transcriptional regulation of *LfF3′H1* and *LfF3′5′H* by LfMYB5, LfMYB113, and LfMYB123.

1 | INTRODUCTION

The regulation of leaf coloration in deciduous trees has long been an enigma. In certain species, leaf coloration occurs in both unexpanded young leaves and senescent leaves, as observed in Formosan sweet gum (*Liquidambar formosana* Hance). Formosan sweet gum is a subtropical deciduous tree species native to Taiwan, and the attractive orange-red to dark red autumn leaf coloration is one of its characteristics. The young unexpanded leaves also present with leaf coloration, but the color produced is more purplish-red to purple. The different color appearances suggest that the contribution of colored compounds may vary with the regulation of biosynthetic genes.

Two major events contribute to autumn leaf coloration: the degradation of chlorophyll and the biosynthesis of anthocyanin (Ougham et al., 2005). Autumn colors are largely caused by anthocyanins (Archetti et al., 2009). The aglycones of anthocyanins are anthocyanidins that can be classified into three types: red cyanidin, brick-red pelargonidin, and purple-blue delphinidin, which differ in hydroxylation at the 3′ site or at the 3′ and 5′ sites on the B-ring (Holton & Cornish, 1995). It has been found that most of the autumn

colors result from the presence of cyanidin (Ishikura, 1972). The color change of young leaves has been given less attention, but it has been confirmed that in some species the contribution of the anthocyanin compounds can differ between unexpanded and senescent leaves (Ishikura, 1972; Yoshitama et al., 1972).

The production of cyanidin, pelargonidin, and delphinidin depends on two mechanisms that have been studied in terms of flower color production (Tanaka et al., 2010). First, the modification of flavanones and dihydroflavonols by FLAVONOID 3′ HYDROXYLASE (F3′H) (EC 1.14.14.82) and FLAVONOID 3′5′ HYDROXYLASE (F3′5′H) (EC 1.14.14.81) occurs to form dihydroflavonols; for example, the *F3′5′H* transgenic rose (*Rosa hybrid*) has blue flowers, due to the accumulation of delphinidin (Tanaka et al., 2010). Second, DIHYDROFLAVONOL-4-REDUCTASE (DFR) (EC 1.1.1.234) may accept certain types of dihydroflavonols as substrates to form the corresponding leucoanthocyanidin products. The substrate preference or specificity of DFRs has been investigated in several plants, including *Petunia* and *Gerbera*, as *Petunia* does not produce orange flowers because its DFR fails to catalyze dihydrokeampferol (Johnson et al., 1999). In addition, it has been confirmed that a single amino acid can change the substrate specificity (Johnson et al., 2001). It was also found that when plants possess more than two DFR genes, the two DFR resulting enzymes may possess different substrate specificities (Hua et al., 2013; Xie et al., 2004). Thus, the two DFRs may contribute to different anthocyanidin products and influence the color.

Plants require sophisticated regulatory mechanisms to ensure that the degree and contribution of anthocyanin pigmentation is appropriate to the large variety of developmental and environmental signals (Albert et al., 2014). Anthocyanin biosynthesis is regulated by the MYB-bHLH-WD40 complex (MBW complex), which consists of two MYBs, two bHLHs, and one WD40 transcription factor (Albert et al., 2014; Gonzalez et al., 2008; Petroni & Tonelli, 2011). Because overexpression of anthocyanin-specific R2R3-MYB genes can promote anthocyanin biosynthesis and the loss-of-function mutant has a distinct phenotype, investigation of anthocyanin biosynthesis regulators in several crop, flower, and fruit plants has become the focus of research. (Borevitz et al., 2000; Cone et al., 1986; Paz-Ares et al., 1987).

In previous studies, the Formosan sweet gum leaf transcriptome and microarray gene expression databases were established, and an anthocyanin biosynthesis-related transcription factor *LfMYB113* was identified (Wen et al., 2015; Wen & Chu, 2017). It was confirmed that *LfMYB113* participates in the regulation of anthocyanin biosynthesis in senescent leaves; however, due to low expression in spring, it is unlikely to play a role in the regulation of anthocyanin biosynthesis in unexpanded young leaves (Wen & Chu, 2017). Thus, the participation of other genes in anthocyanin biosynthesis regulation was speculated in expanding young leaves of Formosan sweet gum.

To explore the regulatory mechanisms in anthocyanin-related leaf coloration in young and senescent leaves of Formosan sweet gum, the anthocyanidins were extracted and analyzed using ultrahigh performance liquid chromatography–ion trap mass spectrometry (UHPLC–MS/MS). The dihydroflavonol substrate acceptability of the two DFRs (LfDFR1 and LfDFR2) was illustrated through recombinant proteins. The activity of LfDFRs and the modification of dihydroflavonols by F3′H (LfF3′H1) or F3′5′H (LfF3′5′H) were confirmed using a transient overexpression experiment. Real-time PCR and promoter assays were performed to study the seasonal gene regulation of *LfDFR1*, *LfDFR2*, *LfF3′H1*, and *LfF3′5′H* by *LfMYB5*, *LfMYB113*, and *LfMYB123*. Finally, based on enzyme functions, regulatory relationships, and gene expression, a gene regulatory network was provided.

2 | MATERIALS AND METHODS

2.1 | Plant materials

Leaves were collected from a Formosan sweet gum plant that grows on the campus of Taiwan National University, Taipei, Taiwan (25°01′17.7″N 121°32′10.0″E) (Wen et al., 2015). The tree was considered to be more than 20 years old because it showed reproductive maturity. Leaves were sampled from 5–8 twigs on different south-faced branches in the third or fourth week of the month during the growing seasons, from December 2010 to December 2014. All leaves were collected on sunny days and immediately frozen in liquid nitrogen and stored at −80°C until use.

2.2 | Anthocyanidin identification

The anthocyanin extraction method was performed according to previous studies (Gould et al., 2000; Schaberg et al., 2008). One milliliter of 3M HCl:H_2O:MeOH (1:3:16, v:v:v) at 4°C was added to 0.1 g of frozen and ground Formosan sweet gum leaf sample, vortexed, and incubated at 4°C with rotation for 24 h. For the *Nicotiana benthamiana* leaf sample, 200 μl of the same solution was added to each 0.1 g of fresh weight leaf sample. Then, the sample was extracted with an equal volume of chloroform, mixed with 1/5 volume of 37% HCl, and boiled for 1 h to release the anthocyanidin aglycones (Xie et al., 2006). Compounds were identified using a Dionex UltiMate 3000 (Thermo Scientific) and amaZon speed (Bruker) UHPLC–MS/MS system with a Luna 5 μm C18(2), 250 × 4.6 mm (Phenomenex) column. The analysis method was as described by a previous study (Teixeira et al., 2015). The mobile phase consisted of two solvents: solvent A (acetonitrile) and solvent B (H_2O and 0.1% formic acid). The solvent gradient was applied as follows: 10% A at the beginning, followed by 20% at 15 min, 25% at 25 min, 35% at 33 min, 50% at 38 min, 90% at 43–48 min, and 10% at 50 min. The flow rate was 1 ml min^{-1}. The MS was operated in both negative and positive modes with 4 kV of capillary, 500 V of end plate offset voltage, 45 psi of nebulizer pressure, 9 ml min^{-1} of dry gas, and 250°C of dry temperature. Anthocyanidins were detected by monitoring the elution at 520 nm, and other compounds were monitored through extracted ion chromatograms with corresponding masses. The standards were purchased from Sigma.

2.3 | Gene cloning

All sequences were acquired from the Formosan sweet gum leaf transcriptome database on the Contigviews web server (http://contigviews.csbb.ntu.edu.tw) (Liu, Tseng, et al., 2014), which was built in a previous study (Wen et al., 2015). The full-length transcript was acquired using the RACE system for Rapid Amplification of cDNA Ends (3′-RACE and 5′-RACE) (Invitrogen, Thermo Scientific) and verified using Phanta Super-Fidelity DNA Polymerase (Vazyme). The sequences were cloned into the pGEM-T Easy vector (Promega) and sequenced.

2.4 | Promoter sequence cloning

Genomic DNA (gDNA) used for full-length sequence cloning was extracted using the Plant Genomic DNA Purification Kit (GeneMark). After the gDNA sequences were cloned, primers for genome walking (BD GenomeWalker Universal Kit, BD Biosciences) were designed according to the manufacturer's instructions to obtain the promoter sequences. The gDNA used in the genome walking experiment was extracted using the modified Pine Tree Method (Chang et al., 1993). For each sample, 1 g of the leaves was used, followed by RNA extraction using the same buffer. After two extractions using chloroform:isoamylalcohol (24:1), the supernatant was precipitated with an equal volume of ice-cold isopropanol and then precipitated for 30 min at −20°C. The precipitate was further centrifuged for 10–15 min at 9390*g* at 4°C, and the supernatant was discarded and vacuum-dried. The pellet was dissolved in 1 ml SSTE (1.0 M NaCl, 0.5% sodium dodecyl sulfate (SDS), 10 mM Tris–HCl (pH 8.0), 1 mM EDTA), extracted with chloroform:isoamylalcohol (24:1) and treated with 50 μg RNase A (Viogene). After extraction with chloroform:isoamylalcohol (24:1), the supernatant was subjected to alcohol precipitation and dissolved in sterilized H_2O. The promoter sequence was amplified using Phanta Super-Fidelity DNA Polymerase (Vazyme), cloned into pGEM-T Easy vector (Promega), and sequenced using 3730xl DNA Analyzer (Applied Biosystems).

2.5 | Sequence alignment and phylogenetic tree

Amino acid sequence alignments and phylogenetic tree images were generated using MEGA 6 (Tamura et al., 2013). The sequence alignments were performed using the ClustalW algorithm, and parameters were set as default. The alignment was visualized using GENEDOC software (Nicholas et al., 1996). We used the neighbor-joining method with the bootstrap set as 1000 to visualize an unrooted tree. Accession numbers of the DFR sequences from other species are provided in Table S1. The DFR sequences were chosen based on publications and their functions. The best sequences with the highest hits in the NCBI non-redundant protein sequences (Nr) database of flavonoid hydroxylase were chosen.

2.6 | Recombinant protein assay

The coding regions of *LfDFR1* and *LfDFR2* were constructed on the pET-28a(+) vector (Novagen, Merck) and transformed into *Escherichia coli* C41 strain to produce recombinant proteins. Luria-Bertani (LB) broth (5 ml) was used to incubate the bacteria, and 0.4 mM IPTG was added to induce protein expression. The bacteria were grown at 16°C for 20 h, centrifuged, and the pellets were stored at −80°C until use.

The recombinant protein assay was performed according to the methods used for GbDFRs (*Ginkgo biloba* L.) and MtDFRs (*Medicago truncatula* Gaertn.) (Hua et al., 2013; Xie et al., 2004). In brief, the pellet was re-suspended in 200 μl lysis buffer (100 mM Tris–HCl, pH 8.0; 5 mM ethylenediaminetetraacetic acid [EDTA], pH 8.0; 100 μg ml^{-1} lysozyme). For citrate/phosphate buffer, Tris–HCl was replaced with citrate/phosphate and incubated at 25°C with gentle shaking. The lysate was sonicated, centrifuged, and the supernatant was transferred to a new tube for the protein assay. The DFR protein reaction assay contained 370 μl Tris–HCl (pH 7.0), 70 μl supernatant, 10 μl substrate, and 50 μl β-nicotinamide adenine dinucleotide 2′-phosphate (NADPH) reduced tetrasodium salt hydrate, and incubated at 30°C for 30 min. Ethyl acetate (EA, 1 ml) was added and centrifuged at 10 000 *g* for 2 min. The supernatant was collected, dried with nitrogen, and stored at 4°C until analysis. The substrate, (±)-dihydrokaempferol, dihydromyricetin, or (±)-taxifolin hydrate (dihydroquercetin), was dissolved in methanol (10 μg μl^{-1}). NADPH was dissolved in 0.01 M NaOH. The substrate and NADPH were purchased from Sigma-Aldrich.

2.7 | Gene expression

Total RNA was extracted using the pine tree method (Chang et al., 1993). In brief, 0.2 g of leaf sample was ground in liquid nitrogen and 2 ml hot extraction buffer (65°C) was added. After extraction twice with chloroform:isoamylalcohol (24:1) (Sigma-Aldrich), the supernatant was precipitated with LiCl at 4°C overnight and centrifuged the next day. The pellet was dissolved in nuclease-free water and the integrity was analyzed using formaldehyde–agarose gel electrophoresis. Approximately 10 μg of the total RNA from each sample was treated with DNase I (Ambion), followed by alcohol precipitation. For each set of samples (same tree in the same year), the first-strand cDNA was synthesized with 1–2.5 μg of purified RNA using SuperScript III Reverse Transcriptase (Invitrogen), followed by rapid amplification of cDNA ends using the 3′-RACE System (Invitrogen). Real-time PCR was performed using Power SYBR Green Master Mix (Applied Biosystems) and a QuantStudio 12K Flex Real-Time PCR System (Applied Biosystems). Formosan sweet gum actin gene, *LfActin2* (GenBank accession No. JX944783) served as the control. All primers used in real-time PCR are listed in Table S2. The samples from March to December (10 months) of the same year are used as a group, and the March samples were used as control. The relative quantification values from each group were calculated separately, and the average values of each mouth from three groups were presented.

2.8 | Transient expression

For LfDFRs, LfF3H, LfF3′Hs, and LfF3′5′H enzyme activity assay, the sequence of *LfDFR1*:His, *LfDFR2*:His, *LfF3H*:His, *LfF3′H1*:His, *LfF3′H2.1*:His, and *LfF3′5′H*:His was constructed into the pBI121 vector (Clontech Laboratories) (Chen et al., 2003). For the promoter assay, the coding sequences of *LfMYB113*, *LfMYB5*, and *LfMYB123* were constructed into the pBI121 vector. The promoter sequences of *LfF3′H1* and *LfF3′5′H* were constructed into the *pBI121-YFP* vector (modification of pBI121), while the promoter sequence of *LfF3′H2.1* was constructed into pCambia1301-*YFP* (modification of pCambia1301) (Marker Gene Technologies). The insert sequences were amplified using Phanta Super-Fidelity DNA Polymerase (Vazyme) from the cloned sequences and digested. After sequencing, the plasmids were transformed into *Agrobacterium tumefaciens* strain GV3101 using the heat shock method.

Gene expression via *agro*infiltration was performed according to a previous study (Wen & Chu, 2017). *N. benthamiana* plants were sown in soil and transferred to a 4-inch plot approximately 10 days after sowing. The plants were grown in a mixture of soil: perlite:vermiculite (3:1:1) and the growth chamber was set to 25°C for 16 h/23°C for 8 h (day/night). Plants were infiltrated in the third week after sowing, and the second to fourth or fifth true leaves were used. *A. tumefaciens* GV3101 strain containing the constructed pBI121 vector colony was transferred into 3–5 ml LB medium (50 mg ml^{-1} gentamycin, 10 mg ml^{-1} rifampicin, and 50 mg ml^{-1} kanamycin), incubated at 28°C, and shaken at 240 rpm overnight. Next, 100 μl of the incubated liquid was transferred to 10 ml LB medium containing 10 mM morpholinoethanesulphonic acid (MES), pH 5.6, 40 mM acetosyringone (AS), 50 mg ml^{-1} gentamycin, 10 mg ml^{-1} rifampicin, and 50 mg ml^{-1} kanamycin and incubated at 28°C with shaking at 240 rpm overnight. The suspension was centrifuged and re-suspended in infiltration buffer (10 mM $MgCl_2$ and 150 mM AS in sterilized H_2O) and incubated at room temperature (25–28°C) for 3 h prior to injection into *N. benthamiana* leaves.

The DFRs, F3H, F3′Hs, and F3′5′H enzyme activity assay was performed according to a previous study (Lau & Sattely, 2015). pBI121-*YFP* (35S::*YFP*) was used as a negative control. Further, 100 μM of the precursors was prepared in methanol with 0.1% DMSO and injected into the *N. benthamiana* leaves on the fourth day after *LfDFR*, *LfF3H*, *LfF3′H*, *LfF3′5′H*, or *YFP* was injected. The leaves were collected on the fifth day, and anthocyanidins were extracted and analyzed as described above. For the promoter assay, a pBI121 empty vector (35S::*GUS*) was used as a negative control and a *pBI121-YFP* (35S::*YFP*) vector was used as a positive control. Images of the leaves were observed under a Canon 350D camera equipped with X-Loupe Agile Lite Box on the third day after injection. All transient overexpression experiments were carried out twice, similar results were obtained, and one of them was presented.

3 | RESULTS

3.1 | Delphinidin and cyanidin are the anthocyanin aglycones in Formosan sweet gum leaf

Leaves of Formosan sweet gum usually start sprouting from late February to early March and continue until April in Taiwan. The sprouts are purplish-red, their color fade as the leaves expand. In contrast, senescent leaves begin to accumulate orange-red to red color in late October until the leaves fall in February. Two anthocyanin aglycones (anthocyanidins) were found in the colored leaves of Formosan sweet gum, namely delphinidin and cyanidin (Figure 1). Purplish-red sprouting leaves had a higher content of delphinidin than cyanidin (Figure 1A). In contrast, the leaves harvested near falling possessed a mottled orange-red to dark red color, with relative cyanidin content higher than that of delphinidin (Figure 1A). From 2011 to 2014, the young leaves collected in late March had a higher content of delphinidin than cyanidin (Figure 1B). In late December, the relative content of these two aglycones differed within sampling; however, a higher content of cyanidin was found in red leaves (Figure 1C). Due to the different colors of delphinidin and cyanidin, the relative content of these two aglycones may cause the color of young and senescent leaves to be different.

3.2 | Substrate acceptability of LfDFR1 and LfDFR2

The contribution of the relative content of the two anthocyanin aglycones might be controlled by biosynthesis. The expression of anthocyanin synthetic enzyme genes was observed using previously generated microarray data (Wen et al., 2015). After identification of the sequences (Wen & Chu, 2017), we found two *LfDFR*s expressed in a different pattern. *LfDFR1* was mainly expressed in April when the leaves were young, while *LfDFR2* was mainly expressed in December when the leaves underwent senescence. We analyzed the amino acid sequences to investigate the activity of LfDFR1 and LfDFR2. Both LfDFR1 and LfDFR2 have conserved NADPH domains and are highly conserved throughout the sequence with the DFRs from other species (Figure S1A). Position 134 is of particular interest because substrate acceptability can be partially predicted and classified based on this position (Hua et al., 2013; Miosic et al., 2014). Position 134 of both LfDFR1 and LfDFR2 contains asparagine (Asn, N), implying that they may accept dihydroquercetin (DHQ) and dihydromyricetin (DHM) as substrates; however, whether dihydrokeampferol (DHK) can be accepted or not remains elusive. In the phylogenetic tree, the two LfDFRs separated into two clades, which, unlike the DFRs of the same species, form a clade as seen in *Populus trichocarpa*, model legume (*Medicago truncatula*), or *Ginkgo biloba* (Figure S1B). LfDFR1 and LfDFR2 were expressed by *E. coli* C41 strain and the crude recombinant protein was used in the *in vitro* assay. We found that both LfDFR1 and LfDFR2 possessed the activity to produce

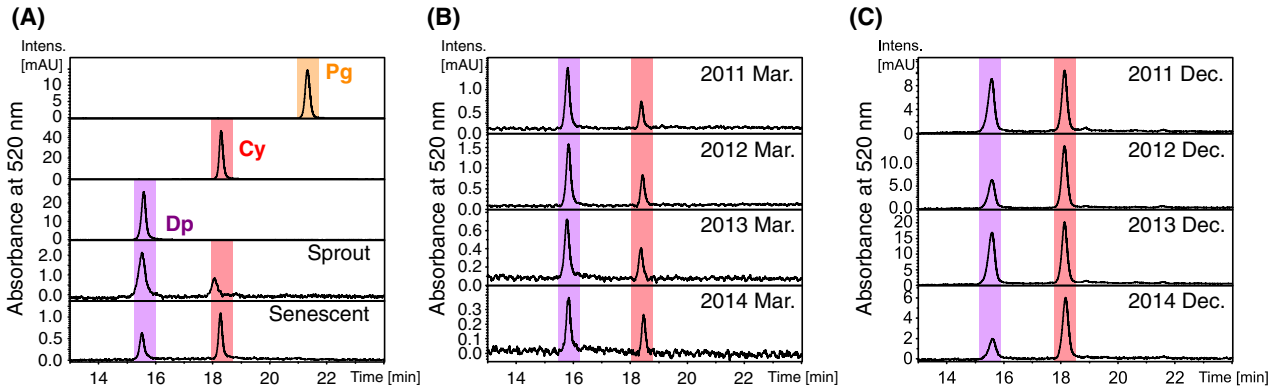

FIGURE 1 Identification of anthocyanin aglycones in Formosan sweet gum colored leaf extract. Ultra-high performance liquid chromatography–mass spectrometry (UHPLC–MS) chromatograms showed the presence of anthocyanin aglycones at 520 nm; the compounds were identified by comparing with the mass spectra of the standards. (A) Anthocyanin standards, sprout leaf samples, and senescent leaf samples. Pg, pelargonidin; Cy, cyanidin; Dp, delphinidin. The sprout leaf and senescent leaf samples were collected in March 2013 and February 2012, respectively. (B) Young leaf samples collected in late March from 2011 to 2014. (C) Senescent leaf samples collected in late December from 2011 to 2014. The colors represent the colors of these compounds. Intens., intensity

leucopelargonidin (Figure S1C, peaks 1 and 2). An unknown product was found in the LfDFR2 assay (Figure S1C, peak 3), which might be an isomer of leucopelargonidin. Both LfDFRs showed no activity with DHQ, DHM, or quercetin (Q), even when pH and temperature were adjusted (Figure S2). The activity of LfDFRs in the *in vitro* assay was inconsistent with the fact that both delphinidin and cyanidin but not pelargonidin were accumulated in the leaves of Formosan sweet gum (Figure 1). The two LfDFR1 and LfDFR2 were then transiently overexpressed in *Nicotiana benthamiana* to observe their activities *in planta*. When *LfMYB113* was used as a regulator to induce the production of endogenous precursors, only delphinidin was found regardless of whether *LfMYB113* is alone or coupled with LfDFR1 or LfDFR2. Thus, the accumulation of delphinidin was speculated to result from the endogenous anthocyanin biosynthetic pathway in *N. benthamiana* (Figure 2A). In order to avoid internal interference in plants, DHK, DHQ, and DHM were injected as substrates. When compared with 35S::*YFP* and mock control, the accumulation of pelargonidin, cyanidin, and delphinidin indicated that both LfDFRs were able to reduce DHK, DHQ, and DHM (Figure 2B, C, D and E), suggesting they play a role as non-specific DFRs. Therefore, if the dihydroflavonol precursors exist and the two LfDFRs can react with the dihydroflavonol precursors, it is assumed that the corresponding leucoanthocyanidin products should be produced and anthocyanidins could be found. It was thus speculated that the production of the dihydroflavonol precursors might affect the contribution of anthocyanidins in the leaves of Formosan sweet gum.

3.3 | The activity of LfF3H, LfF3′H1, LfF3′H2, and LfF3′5′H

To analyze the biosynthesis of dihydroflavonol precursors in Formosan sweet gum, the activities of F3H, F3′H, and F3′5′H were investigated. LfF3H is the only putative F3H gene in the leaf transcriptome database of Formosan sweet gum, which is highly expressed in both April and December (Wen et al., 2015). Three contigs were predicted as putative F3′H genes, among which *LfF3′H1* and *LfF3′H2* have expression patterns similar to those of *LfDFR1* and *LfDFR2*, with the exception of *LfF3′H1*, which also exhibits high expression in December (Wen et al., 2015). After gene cloning, it was shown that *LfF3′H2* had at least two homologs, which differed by only 12 bases and two amino acids, named *LfF3′H2.1* and *LfF3′H2.2*, respectively. The only putative F3′5′H gene, *LfF3′5′H*, showed an expression pattern similar to that of *LfDFR1*, which was high in April when the leaves were not fully expanded (Wen et al., 2015). Phylogenetic analysis (Figure S3) revealed that LfF3H, LfF3′H1, and LfF3′5′H were separated into three clades with their best hits in the NCBI Nr database and the F3H clade formed an outgroup. LfF3′H2.1 and LfF3′H2.2 formed a clade beside F3′H and F3′5′Hs and the functions of the members in this clade are diverse (Figure S3).

The activities of LfF3H, LfF3′H1, LfF3′H2, and LfF3′5′H were analyzed using a transient overexpression assay in leaves of *N. benthamiana*. When naringenin was provided as a precursor (Figure 3A), a strong signal of DHK was found in 35S::*LfF3H*:*His*, while a trace signal was found in *35S::LfF3′5′H:His* (Figure 3B). The data suggested that LfF3H possessed 3′-hydroxylation activity. The signal of eriodictyol (5,7,3′,4′-tetra-hydroxy-flavanone) was found in both 35S::*LfF3′H1*:*His* and 35S::*LfF3′5′H*:*His* (Figure 3B), indicating that both *LfF3′H1* and *LfF3′5′H* had the ability to modify the hydroxylation of the 3′-position. In addition, trace amounts of DHQ were found when *LfF3′H1* was overexpressed, while 5,7,3′,4′,5′-penta-hydroxy-flavanone was found when *LfF3′5′H* was overexpressed (Figure 3C). The transient overexpression assay showed that LfF3H, LfF3′H1, and LfF3′5′H were consistent with their predicted activity. Overexpression of *LfF3H*, *LfF3′H1*, *LfDFR1*, or *LfDFR2* resulted in trace amounts of cyanidin when naringenin was provided as a precursor (Figure 3D), whereas no delphinidin signal was found upon overexpression of *LfF3H* and *LfF3′5′H*, even if coexpress with *LfDFR1* or *LfDFR2* (data not

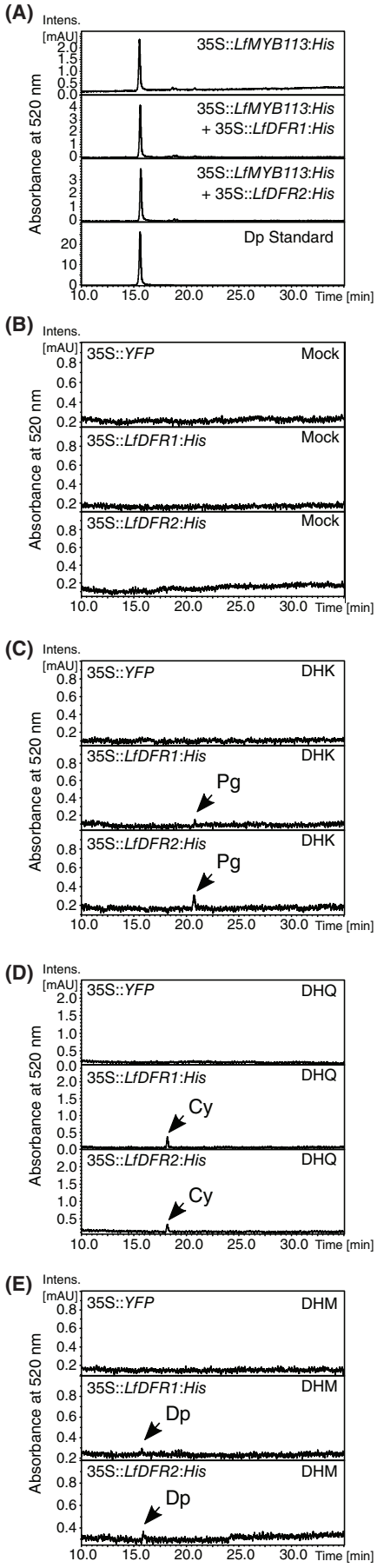

provided). A possible explanation may be the low activity of LfF3′5′H in *N. benthamiana*, as no DHM signal was detected (Figure S4). In contrast to LfF3′H1, no hydroxylation activity was observed for LfF3′H2.1 (Figure S5), suggesting that *LfF3′H2.1* might not play a role in the hydroxylation.

3.4 | The regulation of *LfF3′H1*, *LfF3′5′H*, and *LfDFRs* by LfMYBs

Since LfF3H, LfF3′H1, and LfF3′5′H catalyzed the function of naringenin, which is consistent with their predicted activity, it was speculated that the regulation of anthocyanidin biosynthesis might influence the expression of these genes. Since the anthocyanin-specific MYB gene *LfMYB113* is expressed only when leaves undergo senescence (Wen & Chu, 2017), two other anthocyanin biosynthesis-related R2R3 MYBs were chosen based on their high expression in April, which were recorded in the Formosan sweet gum microarray database (Wen et al., 2015). These two MYB genes were named *LfMYB5* and *LfMYB123*, which were in accordance with the MYB genes from Arabidopsis in reciprocal BLAST. In the phylogenetic analysis, LfMYB5 was located near subgroup 6, composed of anthocyanin biosynthetic regulators (Figure S6). In contrast, LfMYB123 formed a subclade with AtMYB5 and was located near AtMYB123 (Figure S6), suggesting that it might have a role in the regulation of proanthocyanin biosynthesis. For the follow-up experiments, the proanthocyanin-related bHLH transcription factor Transparent Testa 8 (TT8) homolog was acquired based on reciprocal BLAST and named *LfTT8*.

Gene expression of *LfMYB5* and *LfMYB123* was further investigated using real-time PCR of the samples collected from 2012 to 2014. The gene expression patterns of *LfMYB5* and *LfMYB123* (Figure 4A,B) were higher in expanding leaves, while that of *LfMYB113* was higher in senescent leaves (Wen & Chu, 2017). Gene expression of *LfTT8* showed a pattern similar to that of *LfMYB123* (Figure 4C). The expression pattern of *LfF3′H1* suggested *LfMYB5* had

FIGURE 2 Enzyme activities of LfDFR1 and LfDFR2 in transient overexpression experiments in *Nicotiana benthamiana*. Ultra-high performance liquid chromatography–mass spectrometry (UHPLC–MS) chromatograms of assays from transient overexpression of pBI121-*LfDFR1*:*His* or pBI121-*LfDFR2*:*His* in leaves of *N. benthamiana*. pBI121-*YFP* (35S::*YFP*) was used as a negative control. Dihydrokeampferol, dihydromyricetin, and dihydroquercetin were injected as precursors on the fourth day after injection of *Agrobacteria* and leaves were collected 24 h after the precursor injection. The compounds were observed at 520 nm and identified by comparing with the mass spectra of the standards. (A) Overexpression of anthocyanin biosynthetic transcription factor *LfMYB113* or co-expression with one of the *LfDFR*s. (B) Methanol and H_2O were injected as mock. (C) Dihydrokeampferol (DHK) was injected as precursor. Pg, pelargonidin. (D) Dihydroquercetin (DHQ) was injected as precursor. Cy, cyanidin. (E) Dihydromyricetin (DHM) was injected as precursor. Dp, delphinidin. Intens., intensity

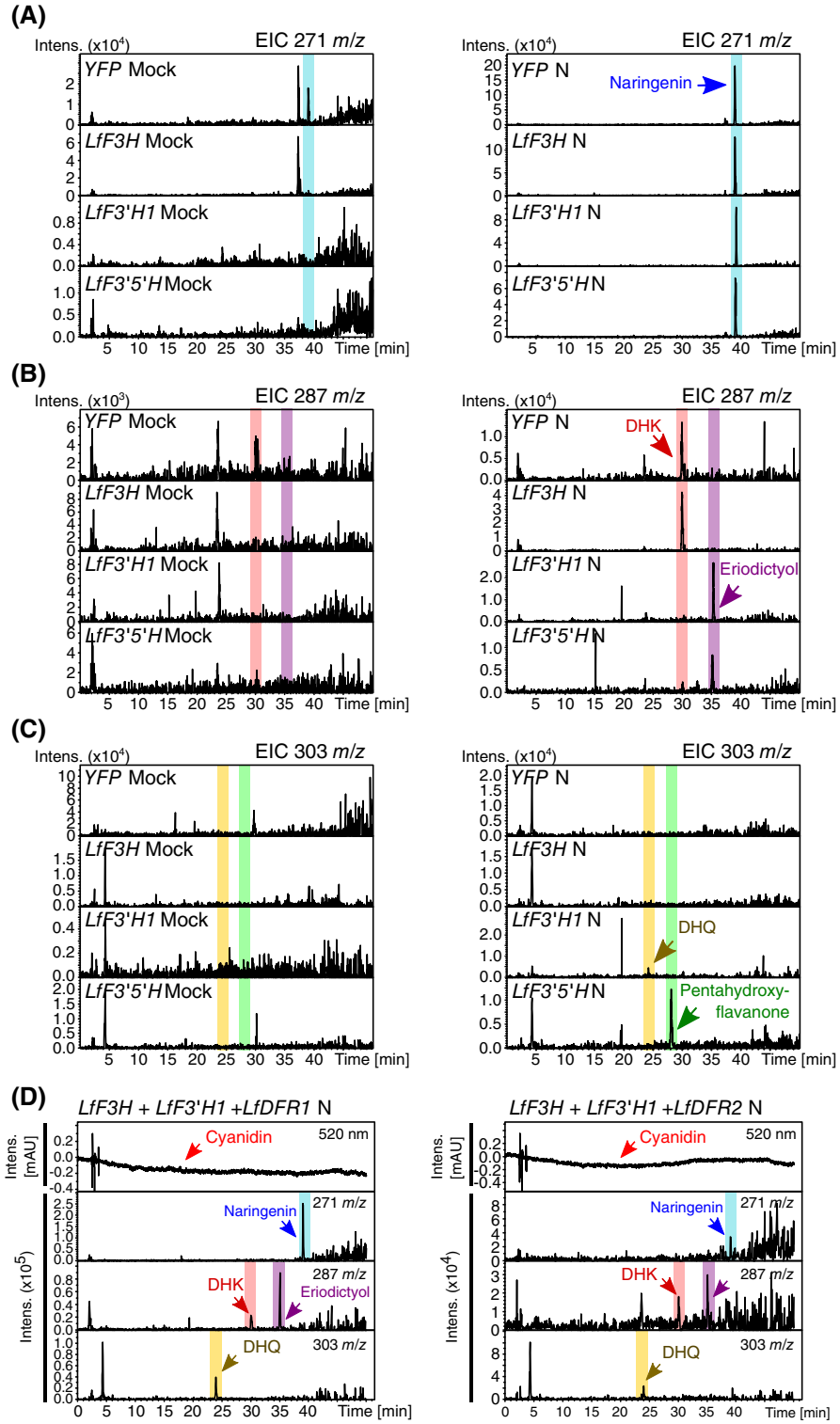

FIGURE 3 Enzyme activities of LfF3H, LfF3′H1, and LfF3′5′H in transient overexpression experiments in *Nicotiana benthamiana*. Ultra-high performance liquid chromatography–mass spectrometry (UHPLC–MS) chromatograms of assays from transient overexpression of *LfF3H*, *LfF3′H1*, or *LfF3′5′H* in leaves of *N. benthamiana*. pBI121-*YFP* (35S::*YFP*) was used as a negative control. Naringenin (N) was injected as a precursor on the fourth day after injection of *Agrobacterium*, and leaves were collected 24 h after precursor injection. Naringenin was replaced with MeOH and injected as a control (mock). The difference in trace signals between the mock might result from the reaction of recombinant proteins and endogenous substrates. The compounds were observed using an extracted ion chromatogram (EIC) and identified using the mass spectra. (A) EIC = 271 *m/z*, screen for naringenin (highlighted in blue). (B) EIC = 287 *m/z*, screen for dihydrokeampferol (DHK) (highlighted in pink), and eriodictyol (highlighted in purple). (C) EIC = 303 *m/z*, screen for dihydroquercetin (DHQ) (highlighted in yellow), and penta-hydroxy-flavanone (highlighted in green). (D) Transient overexpression of *LfF3H*, *LfF3′H1*, and *LfDFR1* (left panel) or *LfDFR2* (right panel). Naringenin was provided as a precursor. The color shades do not represent the color of the compound. Intens., intensity

a regulatory relationship with *LfMYB123* in young leaves and with *LfMYB113* in senescent leaves (Figure 4D). *LfF3′5′H* was expressed at higher levels in young leaves (Figure 4E), and it was unlikely to be regulated by *LfMYB113*. In a previous study, it was confirmed that both *LfDFR1* and *LfDFR2* were regulated by *LfMYB113* (Wen & Chu, 2017). The high expression of *LfDFR1* in April implied the presence of another MYB regulating the process in young leaves (Figure 4F); however, this MYB might not regulate *LfDFR2* (Figure 4G). The high expression of *ANTHOCYANIN SYNTHASE* (*LfANS*) (EC1.14.20.4) in both young and senescent leaves suggested an anthocyanin biosynthetic flow at these two stages (Figure 4H).

The regulatory relationships between these MYB genes and biosynthetic genes were then tested using a transient overexpression assay. It was shown that unlike the activity of *LfMYB113* (Wen &

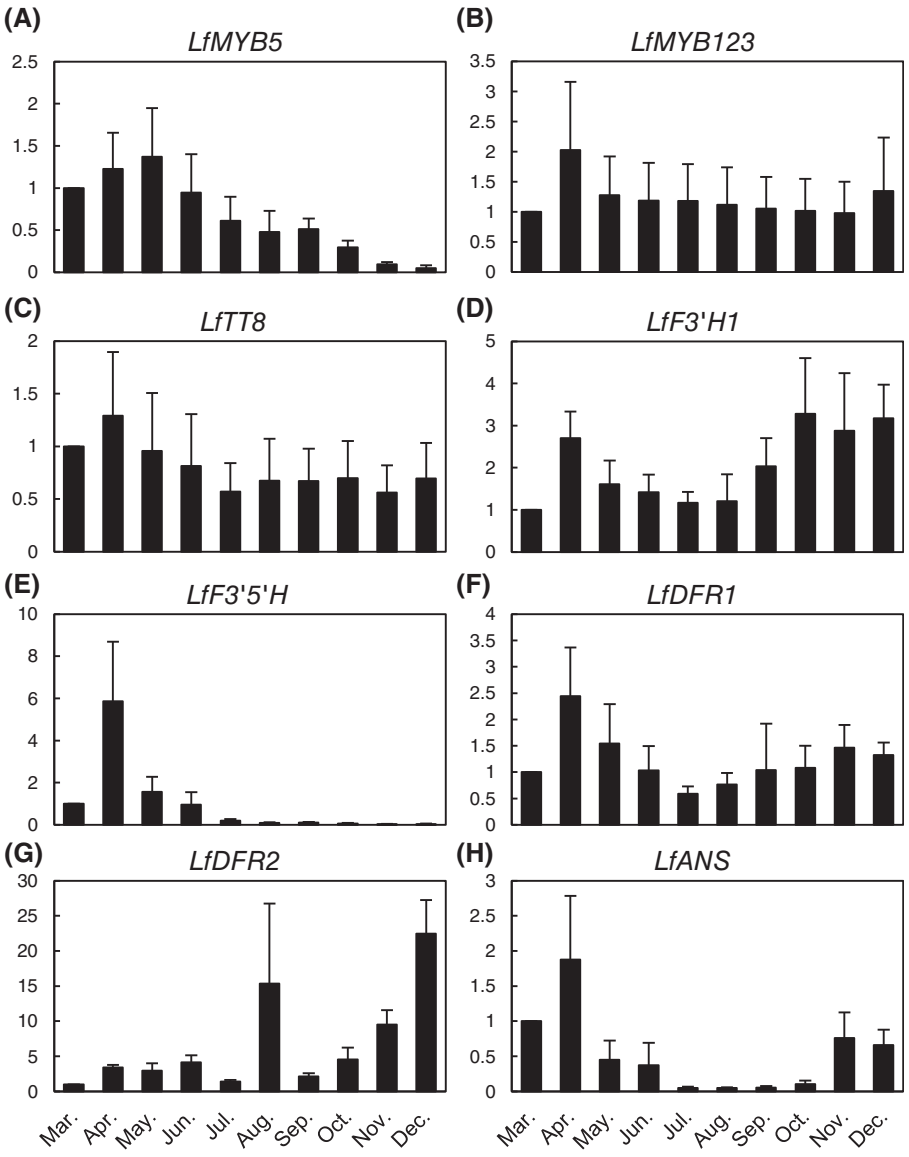

FIGURE 4 Real-time PCR data of anthocyanin biosynthetic-related genes in Formosan sweet gum. Bar charts show the average relative quantification value from 2012 to 2014 generated using real-time PCR. The error bar represents the standard error of the relative quantification value of the 3 years (n = 3). (A) *LfMYB5*, (B) *LfMYB123*, (C) *LfMYB113*, (D) *LfF3′H1*, (E) *LfF3′5′H*, (F) *LfDFR1*, (G) *LfDFR2*, and (H) *LfANS*

Chu, 2017), overexpression of *LfMYB123* promoted the expression of pro*LfDFR1*::*YFP*; however, this depended on co-expression of the bHLH transcription factor *LfTT8* (Figure S7). Co-expression of *LfTT8* with *LfMYB113* showed low promoting activity in pro*LfDFR1* compared to that of *LfMYB123* (Figure S7), suggesting that *LfTT8* is the partner of *LfMYB123* and not *LfMYB113*. *LfMYB123* may not interact with endogenous bHLH genes in *N. benthamiana*. In contrast to pro*LfDFR1*::*YFP* activity, co-expression of *LfMYB123* and *LfTT8* showed weak promoting activity against pro*LfDFR2*::*YFP* (Figure S7). There was no sign that pro*LfDFR1*::*YFP* or pro*LfDFR2*::*YFP* was induced when *LfMYB5* was overexpressed only or co-expressed with *LfTT8* (data not shown), but we could not rule out the possibility that other bHLH genes might be involved, thus whether *LfMYB5* was driving *LfDFR1* or *LfDFR2* was uncertain. Similar to its regulatory relationship with *LfDFR1*, it was clear that *LfMYB113* could promote the expression of *LfF3′H1*, as a strong YFP signal appeared in the transient overexpression assay (Figure 5A). While overexpression of *LfMYB5* did not promote pro*LfF3′H1*::*YFP* (Figure 5B), co-expression of *LfMYB123*, *LfTT8*, and pro*LfF3′H1*::*YFP* showed strong YFP signal (Figure 5C). The promoting activity of *LfMYB123* toward pro*LfF3′H1*::*YFP* was dependent on co-expression of *LfTT8*. In contrast to the prediction from *LfF3′5′H* gene expression data, *LfMYB113* showed positive regulation of pro*LfF3′5′H*::*YFP* (Figure 6A). In contrast to the regulation of pro*LfF3′H1*::*YFP*, pro*LfF3′5′H*::*YFP* was induced by *LfMYB5* (Figure 6B) but not *LfMYB123* (Figure 6C). In summary, *LfMYB5* promotes the expression of pro*LfF3′5′H*::*YFP*, whereas *LfMYB123* promotes the expression of pro*LfF3′H1*::*YFP*, and *LfMYB113* promotes the expression of both pro*LfF3′H1*::*YFP* and pro*LfF3′5′H*::*YFP*.

4 | DISCUSSION

The biosynthesis and regulation of anthocyanin have been studied extensively in several plants, from flowers to crops and fruits (Albert et al., 2014; Allan et al., 2008; Petroni & Tonelli, 2011; Tanaka

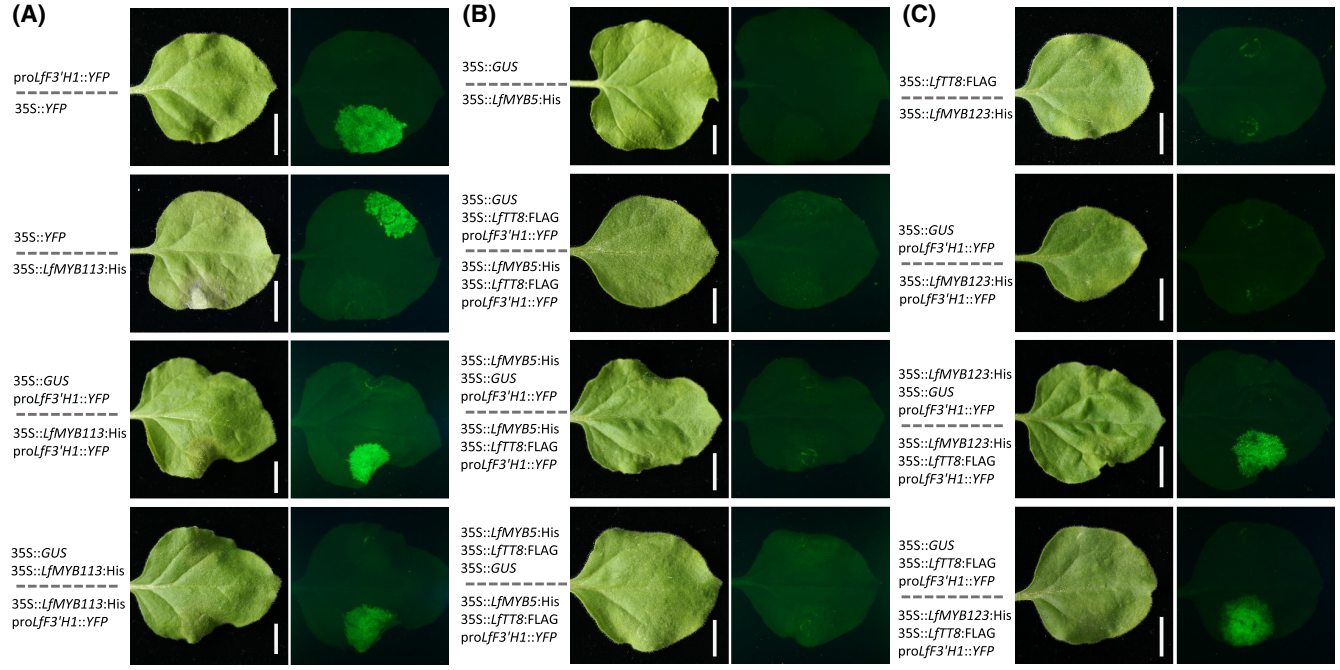

FIGURE 5 Transient overexpression assay of *LfMYB113*, *LfMYB5*, and *LfMYB123* in promoting the expression of pro*LfF3′H1*::*YFP*. Transient overexpression of (A) *LfMYB113*, (B) *LfMYB5*, or (C) *LfMYB123* as an activator to promote the expression of pro*LfF3′H1*::*YFP*. The genes were constructed using the pBI121 vector, the empty vector was used as a negative control (35S::*GUS*), and the *YFP gene* was used as a positive control (35S::*YFP*). Each construct was grown separately and mixed before injection into the leaves of *Nicotiana benthamiana*. The construct names above or under the dashed line on the left of the photo were the Agrobacterium injected to the right or left of the middle rib. The photo on the left shows the appearance of the leaf, and the photo on the right shows the YFP signal under the X-Loupe Agile Lite Box. The white scale bar represents 1 cm

et al., 2010; Winkel-Shirley, 2001). However, there is limited information on the contribution of anthocyanin aglycones in vegetative organs, as is the accumulation of delphinidin and cyanidin in two different developmental stages of the same tissue. The contribution of anthocyanidins in these two developmental stages reveals the different regulatory pathways in these two stages. Interestingly, although the biosynthetic pathway is quite conserved, the causes that affect the appearance of color through anthocyanin biosynthesis may vary in different species (Tanaka et al., 2010). We identified that leaf coloration is controlled by the regulation of gene expression and not by enzyme activity. In this study, it was found that there were two types of anthocyanidins in young and senescent leaves of Formosan sweet gum; the relative amount was different in these two developmental stages, and it was regulated by the gene expression of *LfF3′H1* and *LfF3′5′H*.

4.1 | Regeneration of anthocyanins in the leaves of Formosan sweet gum

In this study, delphinidin and cyanidin were found to be the two types of anthocyanidins in leaves of Formosan sweet gum; the relative amounts of delphinidin and cyanidin were different in young and senescent leaves (Figure 1). The contribution of anthocyanin glycosides and aglycones in young leaves of *Acer* species differs from that in autumn leaves (Ishikura, 1972). Different types of anthocyanins suggested that the anthocyanins in autumn leaves were newly synthesized. The lack of anthocyanins in summer green leaves of nine red-senescing species (*Acer rubrum*, *Acer saccharum*, *Cornus alternifolia*, *Fraxinus americana*, *Prunus serotine*, *Quercus rubra*, *Vaccinium corymbosum*, *Viburnum alnifolium*, and *Viburnum cassinoides*) indicates that they are newly synthesized in autumn leaves (Lee et al., 2003). Consistent with previous research, measurements of the absorbance at 530 nm indicated that the content of anthocyanin in summer is low and that the content in the young leaves is relatively lower than that in the senescent leaves of Formosan sweet gum (Wen & Chu, 2017). Although the degradation, modification, or dilution of anthocyanins in young leaves is unknown, identification of newly synthesized anthocyanins in autumn leaf coloration can be performed based on gene regulation. The present work illustrated that the different gene regulators participating in these two developmental stages provided molecular evidence for anthocyanin regeneration in senescent leaves.

4.2 | Anthocyanin biosynthesis-related MYB transcription factors

The anthocyanin-specific R2R3 MYB transcription factors have been recognized as the main regulator responsible for the color in several economic plants, for example, grape (*Vitis vinifera*), apple (*Malus*

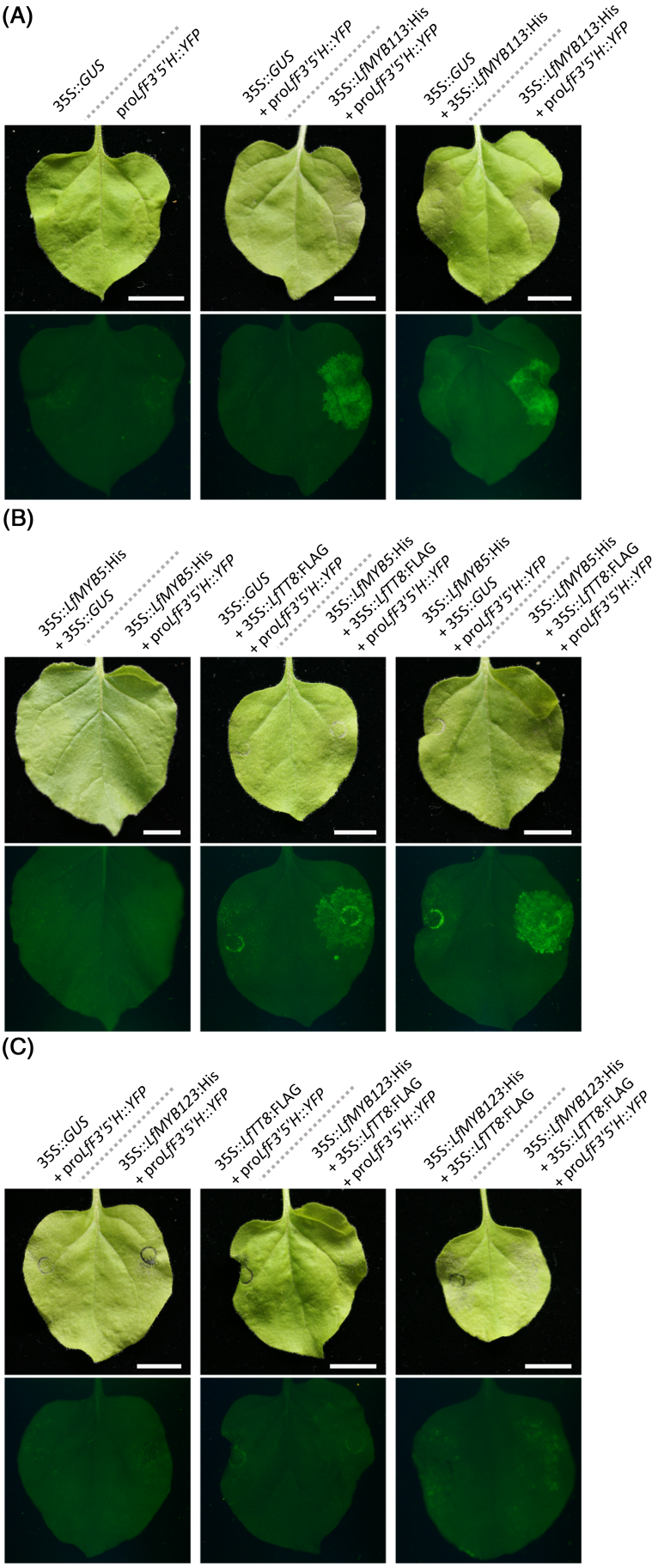

FIGURE 6 Transient overexpression assay of *LfMYB113*, *LfMYB5*, and *LfMYB123* in promoting the expression of pro*LfF3′5′H*::*YFP*. Transient overexpression of (A) *LfMYB113*, (B) *LfMYB5*, or (C) *LfMYB123* as an activator to promote the expression of pro*LfF3′5′H*::*YFP*. The genes were constructed on the pBI121 vector, while the empty vector was used as a negative control (35S::*GUS*) and the *YFP* gene was used as a positive control (*35S::YFP*). Each construct was grown separately and mixed before injection into the leaves of *Nicotiana benthamiana*. The construct names on the left or right of the dashed line above the photo were the *Agrobacterium* injected to the left or right of the middle rib. The photo at the top shows the appearance of the leaf, and the photo at the bottom shows the YFP signal under the X-Loupe Agile Lite Box. The white scale bar represents 1 cm

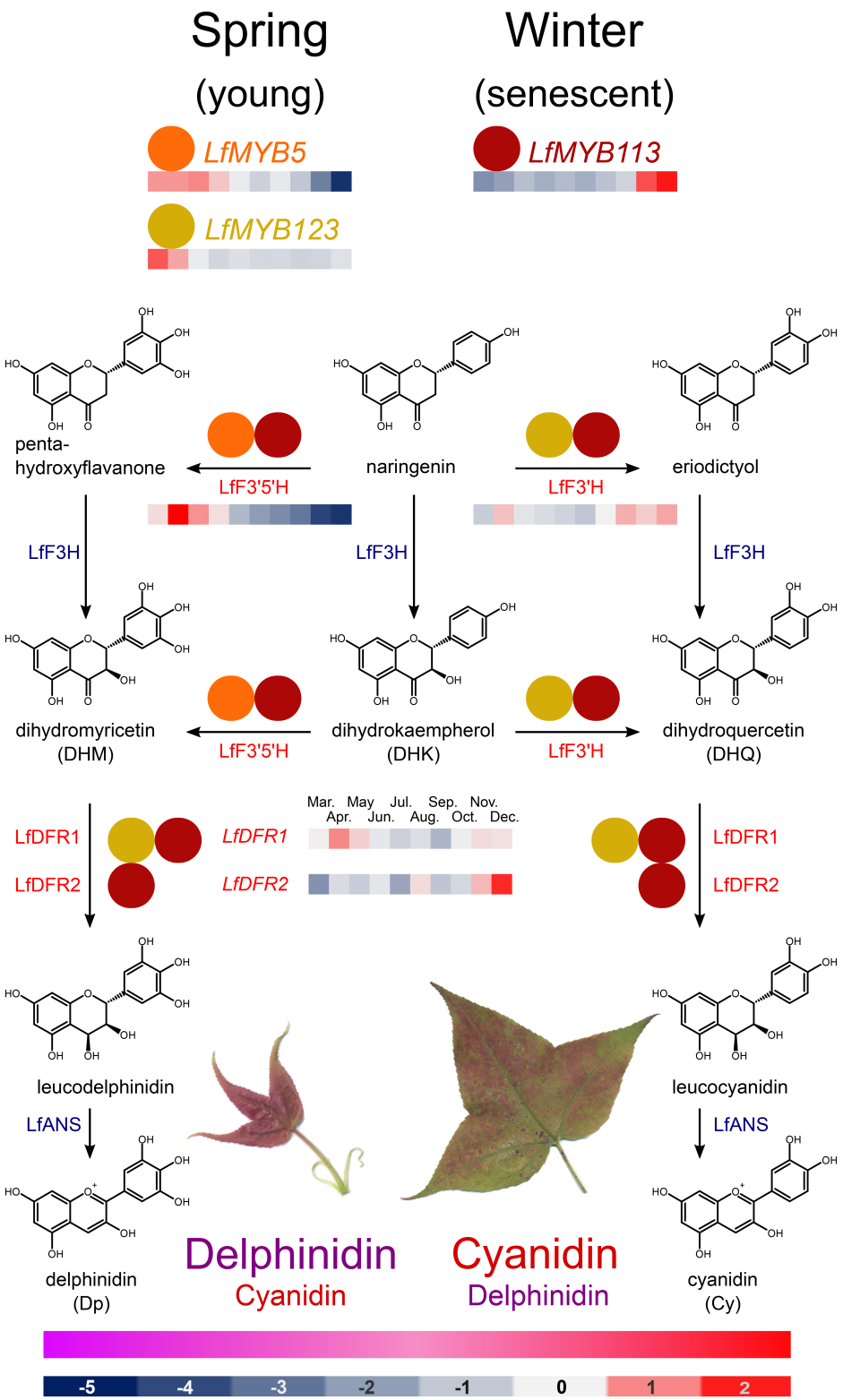

FIGURE 7 Summary of gene regulatory network of anthocyanidin biosynthesis and leaf coloration of Formosan sweet gum. Orange, yellow, and red balls near the enzyme names represent transcriptional regulation by *LfMYB5*, *LfMYB123*, and *LfMYB113* identified in this work. The 10 colored boxes near the MYBs and enzymes represent gene expression data generated using real-time PCR data from Figure 4 with log2-fold change, which correlates to the average of 10 months. Enzyme names are presented in dark blue and the focus of this study is presented in red. The anthocyanin biosynthesis pathway was determined according to the pathway in Arabidopsis (Winkel-Shirley, 2001). Gene expression of *LfMYB113* and the relationships of *LfMYB113* in regulation of *LfDFR1* and *LfDFR2* were according to a previous work (Wen & Chu, 2017). The heatmap color was generated using Microsoft Excel 2016 and edited with Inkscape software. The colors under delphinidin and cyanidin represent the colors of these compounds

domestica), sweet potato (*Ipomoea batatas*), tomato (*Solanum lycopersicum*), pepper (*Capsicum annuum*), petunia (*Petunia* × *hybrida*), and snapdragon (*Antirrhinum majus*) (Allan et al., 2008). In certain plants, more than one anthocyanin-specific MYBs are present and can be partially redundant or participate in different tissues. In Arabidopsis, *AtMYB75/PAP1*, *AtMYB90/PAP2*, *AtMYB113*, and *AtMYB114* specifically regulate anthocyanin biosynthesis. The former two regulate both the early- and late-anthocyanin biosynthetic pathways, whereas the latter two regulate only the late genes (Gonzalez et al., 2008). In apple, the allelic genes *MdMYB1*(*MdMYBA*) and *MdMYB10* were shown to control fruit flesh (*MdMYB10*), foliage anthocyanin pigmentation (*MdMYB10*), and fruit skin color (*MdMYB1*) (Chagné et al., 2013; Lin-

Wang et al., 2010). To date, all published anthocyanin biosynthesis MYBs have been identified to play a role in a single stage of development, such as flowering, fruit ripening, or leaf coloration, which are associated with senescence. The only anthocyanin-specific MYB identified in the Formosan sweet gum leaf transcriptome database is also a senescence regulator (Wen & Chu, 2017); however, the presence of other anthocyanin-specific MYB genes remains unknown. The findings of different MYB genes participating in anthocyanin biosynthetic regulation in different developmental stages of a tissue show that the regulation of anthocyanin biosynthesis may be more complicated than expected.

The two MYB genes that upregulate *LfF3′H*, *LfF3′5′H*, and *LfDFR1* in young leaves were *LfMYB5* and *LfMYB123* (Figures 5, 6, and S7), both of which were predicted to be proanthocyanin-biosynthetic regulators. Proanthocyanidin is derived from the reduction of leucoanthocyanidin and anthocyanidin (Sharma & Dixon, 2005). The *MYB5* homolog has been studied in several plants. In Arabidopsis, *AtMYB5* plays minor roles in proanthocyanin biosynthetic regulation; however, in the model legume, grape, and *Freesia hybrida*, *MtMYB5*, *VvMYB5a*, *VvMYB5d*, and *FhMYB5* regulate both anthocyanin and proanthocyanin biosynthetic genes (Deluc et al., 2006, 2008; Li et al., 2019; Liu, Jun, & Dixon, 2014). Homologs of *LfMYB123* in Arabidopsis are the proanthocyanin regulator *TT2*/*AtMYB123*, which positively regulates *DFR*, *LDOX*, *BANYULS* (*BAN*, also named as *ANTHOCYANIDIN REDUCTASE*), and *TT12* (Nesi et al., 2001). *MtMYB14*, the *TT2* homolog in *Medicago truncatula*, has a limited regulatory role; however, it regulates *LDOX* and *ANR* (Liu, Jun, & Dixon, 2014). In addition, proanthocyanins may play certain roles in young tissues, as it has been shown that *VvMYB5a* is mainly expressed during the early stages of berry development (Deluc et al., 2006). According to the function of these homologs, it was speculated that *LfMYB5* and *LfMYB123* might regulate proanthocyanin biosynthesis. The expression of *LfMYB5* and *LfMYB123* indicates that proanthocyanidins may be highly accumulated in unexpanded young leaves, and the accumulation of anthocyanins may be a side effect of the activation of these genes.

4.3 | Regulatory network of leaf coloration in Formosan sweet gum

The regulation of anthocyanidin biosynthesis in young and senescent leaves in Formosan sweet gum is different (Figure 7). *LfMYB5* induces the expression of *LfF3′5′H*, and *LfMYB123* induces the expression of *LfF3′H1* and *LfDFR1*; the outcome is higher delphinidin content and the young sprouting leaves appearing purplish-red in color. On the other hand, *LfMYB113* induces the expression of *LfF3′H1*, *LfDFR1*, and *LfDFR2* when leaves undergo senescence. The senescent leaves possess orange-red to dark red color, which might be due to the higher content of cyanidin.

Over the past few decades, several studies have focused on different aspects to explain the anthocyanin-related color appearance at the molecular level. Several genes were found by comparison of mutants, phenotypes, varieties, cultivars, and developmental stages. These studies can be classified as studies on biosynthetic and regulatory genes. The former identified F3′5′H mutants (Tanaka et al., 2010) or DFR functions (Hua et al., 2013; Johnson et al., 2001; Xie et al., 2004), which influence anthocyanidin and color, while the latter mainly focus on anthocyanin specific MYB transcription factors including activators (Borevitz et al., 2000; Lin-Wang et al., 2010), repressors (Aharoni et al., 2001; Davies et al., 2012), transposable elements (Butelli et al., 2012), and retrotransposon-induced loss of functional mutants (Kobayashi et al., 2004). In contrast to previous studies, this study focused on both biosynthetic and regulatory genes in two developmental stages of a tissue from an individual plant. It is surprising that both the LfF3′H1 and LfF3′5′H possess predicted functions and the two LfDFRs are non-specific. The functional identification of LfDFRs, LfF3′H, and LfF3′5′H suggested that the gene expression of *LfF3′H1* and *LfF3′5′H* might influence anthocyanidin biosynthesis and thus the leaf color in Formosan sweet gum. In addition, our findings suggest that proanthocyanin biosynthesis regulators participate in anthocyanin biosynthesis in young leaves and that anthocyanin-specific regulators act in senescent leaves; both processes result in anthocyanin accumulation. As a whole, this study provides valuable insights on leaf coloration.

5 | CONCLUSIONS

Gene expression and regulatory relationships of *LfMYB5*, *LfMYB113*, *LfF3′H1*, *LfF3′5′H*, *LfDFR1*, and *LfDFR2* illustrate the regulatory mechanism of anthocyanidin biosynthesis and thus explain the biosynthesis of leaf colors in Formosan sweet gum at different developmental stages. The regulation of gene expression of *LfF3′H1* and *LfF3′5′H* by *LfMYB5*, *LfMYB113*, and *LfMYB123* play a major role in influencing the contribution of anthocyanidins to Formosan sweet gum leaf coloration. This finding provides insights on the regulation of plant anthocyanidin biosynthesis, as multiple MYBs regulate various biosynthetic genes in different developmental stages of the same organ.

ACCESSION NUMBERS

GenBank accession numbers for promoter sequences and genomic DNA sequences of *LfDFR1* and *LfDFR2* are JX975398 and KX902508, respectively. The GenBank accession numbers for the protein sequences of *LfDFR1* and *LfDFR2* are AGT28278 and AQM49951. GenBank accession numbers for full-length transcript sequences of *LfANS* are JX944786.

GenBank accession numbers for full-length transcript sequences of *LfMYB5*, *LfMYB113*, *LfMYB123*, *LfTT8*, *LfF3′H1*, *LfF3′H2*, *LfF3′5′H*, *LfF3H*, and *LfDFR2* are MT435088 to MT435096.

GenBank accession numbers for promoter sequences of *LfF3′H1*, *LfF3′H2*, and *LfF3′5′H* are MT435097, MT435098, and MT435099.

GenBank accession number for *LfActin2* is JX944783.

ACKNOWLEDGMENTS

The authors thank the DNA Sequencing Core Facility (Core Facility and Innovative Instrument Project, AS-CFII-108-115) for their support in DNA Sequencing. The authors are grateful to Dr. Shih-Shun Lin (Institute of Biotechnology, National Taiwan University, Taiwan) for the expert technical advice on infiltration and Mei-Jane Fang (DNA Analysis Core Laboratory, Institute of Plant and Microbial Biology, Academia Sinica, Taiwan) for the expert technical assistance with real-time PCR. This study was funded by the Ministry of Science and Technology, Taiwan.

AUTHOR CONTRIBUTIONS

Chi-Hsiang Wen and Fang-Hua Chu conceived the project. Chi-Hsiang Wen performed most of the experiments and wrote the article with contributions from all the authors. Nai-Wen Tsao performed all the LC/MS experiments and data analysis. Sheng-Yang Wang and Nai-Wen Tsao provided technical assistance to Chi-Hsiang Wen, Sheng-Yang Wang and Fang-Hua Chu supervised the experiments and wrote the article.

CONFLICT OF INTERESTS

The authors declare that they have no conflicts of interest.

DATA AVAILABILITY STATEMENT

The data that support the findings of this study are available from the corresponding author, Prof. F. H. Chu, upon reasonable request.

ORCID

Fang-Hua Chu https://orcid.org/0000-0003-2299-5013

REFERENCES

Aharoni, A., Ric De Vos, C.H., Wein, M., Sun, Z., Greco, R., Kroon, A. et al. (2001) The strawberry FaMYB1 transcription factor suppresses anthocyanin and flavonol accumulation in transgenic tobacco. *The Plant Journal*, 28, 319–332.

Albert, N.W., Davies, K.M., Lewis, D.H., Zhang, H., Montefiori, M., Brendolise, C. et al. (2014) A conserved network of transcriptional activators and repressors regulates anthocyanin pigmentation in eudicots. *Plant Cell*, 26, 962–980.

Allan, A.C., Hellens, R.P. & Laing, W.A. (2008) MYB transcription factors that colour our fruit. *Trends in Plant Science*, 13, 99–102.

Archetti, M., Döring, T.F., Hagen, S.B., Hughes, N.M., Leather, S.R., Lee, D. W. et al. (2009) Unravelling the evolution of autumn colours: an interdisciplinary approach. *Trends in Ecology and Evolution*, 24, 166–173.

Borevitz, J.O., Xia, Y., Blount, J., Dixon, R.A. & Lamb, C. (2000) Activation tagging identifies a conserved MYB regulator of phenylpropanoid biosynthesis. *Plant Cell*, 12, 2383–2394.

Butelli, E., Licciardello, C., Zhang, Y., Liu, J., Mackay, S., Bailey, P. et al. (2012) Retrotransposons control fruit-specific, cold-dependent accumulation of anthocyanins in blood oranges. *Plant Cell*, 24, 1242–1255.

Chagné, D., Lin-Wang, K., Espley, R.V., Volz, R.K., How, N.M., Rouse, S. et al. (2013) An ancient duplication of apple MYB transcription factors is responsible for novel red fruit-flesh phenotypes. *Plant Physiology*, 161, 225–239.

Chang, S., Puryear, J. & Cairney, J. (1993) A simple and efficient method for isolating RNA from pine trees. *Plant Molecular Biology Reporter*, 11, 113–116.

Chen, P.-Y., Wang, C.-K., Soong, S.-C. & To K-Y. (2003) Complete sequence of the binary vector pBI121 and its application in cloning T-DNA insertion from transgenic plants. *CEUR Workshop Proceedings*, 11, 287–293.

Cone, K.C., Burr, F.A. & Burr, B. (1986) Molecular analysis of the maize anthocyanin regulatory locus C1. *Proceedings of the National Academy of Sciences of the United States of America*, 83, 9631–9635.

Davies, K.M., Albert, N.W. & Schwinn, K.E. (2012) From landing lights to mimicry: the molecular regulation of flower colouration and mechanisms for pigmentation patterning. *Functional Plant Biology*, 39, 619–638.

Deluc, L., Barrieu, F.C., Marchive, C., Lauvergeat, V., Decendit, A., Richard, T. et al. (2006) Characterization of a grapevine R2R3-MYB transcription factor that regulates the phenylpropanoid pathway. *Plant Physiology*, 140, 499–511.

Deluc, L., Bogs, J., Walker, A.R., Ferrier, T., Decendit, A., Merillon, J.-M. et al. (2008) The transcription factor VvMYB5b contributes to the regulation of anthocyanin and proanthocyanidin biosynthesis in developing grape berries. *Plant Physiology*, 147, 2041–2053.

Gonzalez, A., Zhao, M., Leavitt, J.M. & Lloyd, A.M. (2008) Regulation of the anthocyanin biosynthetic pathway by the TTG1/bHLH/Myb transcriptional complex in Arabidopsis seedlings. *The Plant Journal*, 53, 814–827.

Gould, K.S., Markham, K.R., Smith, R.H. & Goris, J.J. (2000) Functional role of anthocyanins in the leaves of Quintinia serrata Cunn. A. *Journal of Experimental Botany*, 51, 1107–1115.

Holton, T.A. & Cornish, E.C. (1995) Genetics and biochemistry of anthocyanin biosynthesis. *Plant Cell*, 7, 1071–1083.

Hua, C., Linling, L., Shuiyuan, C., Fuliang, C., Feng, X., Honghui, Y. et al. (2013) Molecular cloning and characterization of three genes encoding dihydroflavonol-4-reductase from *Ginkgo biloba* in anthocyanin biosynthetic pathway. *PLoS One*, 8, 1–16.

Ishikura, N. (1972) Anthocyanin and other phenolics in autumn leaves. *Phytochemistry*, 11, 2555–2558.

Johnson, E.T., Ryu, S., Yi, H., Shin, B., Cheong, H. & Choi, G. (2001) Alteration of a single amino acid changes the substrate specificity of dihydroflavonol 4-reductase. *The Plant Journal*, 25, 325–333.

Johnson, E.T., Yi, H., Shin, B., Oh, B.J., Cheong, H. & Choi, G. (1999) Cymbidium hybrida dihydroflavonol 4-reductase does not efficiently reduce dihydrokaempferol to produce orange pelargonidin-type anthocyanins. *The Plant Journal*, 19, 81–85.

Kobayashi, S., Goto-yamamoto, N. & Hirochika, H. (2004) Retrotransposon-induced mutations in grape skin color. *Science*, 304, 982.

Lau, W. & Sattely, E.S. (2015) Six enzymes from mayapple that complete the biosynthetic pathway to the etoposide aglycone. *Science*, 349, 1224–1228.

Lee, D.W., O'Keefe, J., Holbrook, N.M. & Feild, T.S. (2003) Pigment dynamics and autumn leaf senescence in a New England deciduous forest, eastern USA. *Ecological Research*, 18, 677–694.

Li, Y., Shan, X., Zhou, L., Gao, R., Yang, S., Wang, S. et al. (2019) The R2R3-MYB factor FhMYB5 from Freesia hybrida contributes to the regulation of anthocyanin and proanthocyanidin biosynthesis. *Frontiers in Plant Science*, 9, 1–15.

Lin-Wang, K., Bolitho, K., Grafton, K., Kortstee, A., Karunairetnam, S., TK, M.G. et al. (2010) An R2R3 MYB transcription factor associated with regulation of the anthocyanin biosynthetic pathway in Rosaceae. *BMC Plant Biology*, 10, 50.

Liu, C., Jun, J.H. & Dixon, R.A. (2014) MYB5 and MYB14 play pivotal roles in seed coat polymer biosynthesis in *Medicago truncatula*. *Plant Physiology*, 165, 1424–1439.

Liu, L.-Y.D., Tseng, H.-I., Lin, C.-P., Lin, Y.-Y., Huang, Y.-H., Huang, C.-K. et al. (2014) High-throughput transcriptome analysis of the leafy flower transition of *Catharanthus roseus* induced by peanut witches ' -broom phytoplasma infection. *Plant and Cell Physiology*, 55, 942–957.

Miosic, S., Thill, J., Milosevic, M., Gosch, C., Pober, S., Molitor, C. et al. (2014) Dihydroflavonol 4-reductase genes encode enzymes with contrasting substrate specificity and show divergent gene expression profiles in Fragaria species. *PLoS One*, 9(11), e112707.

Nesi, N., Jond, C., Debeaujon, I., Caboche, M. & Lepiniec, L. (2001) The Arabidopsis TT2 gene encodes an R2R3 MYB domain protein that acts as a key determinant for proanthocyanidin accumulation in developing seed. *Plant Cell*, 13, 2099–2114.

Nicholas, K.B., Nicholas, H.B.J. & Deerfield, D.W.I. (1996) GeneDoc: analysis and visualization of genetic variation. *EMBNEW*, 4, 14.

Ougham, H.J., Morris, P. & Thomas, H. (2005) The colors of autumn leaves as symptoms of cellular recycling and defenses against environmental stresses. *Current Topics in Developmental Biology*, 66, 135–160.

Paz-Ares, J., Ghosal, D., Wienand, U., Peterson, P.A. & Saedler, H. (1987) The regulatory c1 locus of *Zea mays* encodes a protein with homology to myb proto-oncogene products and with structural similarities to transcriptional activators. *The EMBO Journal*, 6, 3553–3558.

Petroni, K. & Tonelli, C. (2011) Recent advances on the regulation of anthocyanin synthesis in reproductive organs. *Plant Science*, 181, 219–229.

Schaberg, P.G., Murakami, P.F., Turner, M.R., Heitz, H.K. & Hawley, G.J. (2008) Association of red coloration with senescence of sugar maple leaves in autumn. *Trees*, 22, 573–578.

Sharma, S.B. & Dixon, R.A. (2005) Metabolic engineering of proanthocyanidins by ectopic expression of transcription factors in *Arabidopsis thaliana*. *The Plant Journal*, 44, 62–75.

Tamura, K., Stecher, G., Peterson, D., Filipski, A. & Kumar, S. (2013) MEGA6: molecular evolutionary genetics analysis version 6.0. *Molecular Biology and Evolution*, 30, 2725–2729.

Tanaka, Y., Brugliera, F., Kalc, G., Senior, M., Dyson, B., Nakamura, N. et al. (2010) Flower color modification by engineering of the flavonoid biosynthetic pathway: practical perspectives. *Bioscience, Biotechnology, and Biochemistry*, 74, 1760–1769.

Teixeira, L.D.L., Bertoldi, F.C., Lajolo, F.M. & Hassimotto, N.M.A. (2015) Identification of Ellagitannins and flavonoids from Eugenia brasilienses lam. (Grumixama) by HPLC-ESI-MS/MS. *Journal of Agricultural and Food Chemistry*, 63, 5417–5427.

Wen, C.-H. & Chu, F.-H. (2017) A R2R3-MYB gene LfMYB113 is responsible for autumn leaf coloration in formosan sweet gum (Liquidambar formosana Hance). *Plant and Cell Physiology*, 58, 508–521.

Wen, C.-H., Lin, S.-S. & Chu, F.-H. (2015) Transcriptome analysis of a subtropical deciduous tree: autumn leaf senescence gene expression profile of Formosan gum. *Plant and Cell Physiology*, 56, 163–174.

Winkel-Shirley, B. (2001) Flavonoid biosynthesis. A colorful model for genetics, biochemistry, cell biology, and biotechnology. *Plant Physiology*, 126, 485–493.

Xie, D., Jackson, L. & Cooper, J. (2004) Molecular and biochemical analysis of two cDNA clones encoding dihydroflavonol-4-reductase from *Medicago truncatula*. *Plant Physiology*, 134, 979–994.

Xie, D.Y., Sharma, S.B., Wright, E., Wang, Z.Y. & Dixon, R.A. (2006) Metabolic engineering of proanthocyanidins through co-expression of anthocyanidin reductase and the PAP1 MYB transcription factor. *The Plant Journal*, 45, 895–907.

Yoshitama, K., Ozaku, M., Hujii, M. & Hayashi, K. (1972) A survey of anthocyanins in sprouting leaves of some Japanese angiosperms studies on anthocyanins, LXV. *Botanical Magazine*, 85, 303–306.

SUPPORTING INFORMATION

Additional supporting information may be found online in the Supporting Information section at the end of this article.

How to cite this article: Wen C-H, Tsao N-W, Wang S-Y, Chu F-H. Color variation in young and senescent leaves of Formosan sweet gum (*Liquidambar formosana*) by the gene regulation of anthocyanidin biosynthesis. *Physiologia Plantarum*. 2021;172:1750–1763. https://doi.org/10.1111/ppl.13385